Res Chem Intermed
DOI 10.1007/s11164-015-1920-x

Fe-amino acid complexes immobilized on silica gel as active and highly selective catalysts in cyclohexene epoxidation

Gábor Varga · Zita Csendes · Éva G. Bajnóczi · Stefan Carlson · Pál Sipos · István Pálinkó

Received: 1 October 2014 / Accepted: 2 January 2015

Abstract In this work, the syntheses, structure, superoxide dismutase (SOD) activity, and the catalytic use in the oxidative transformations of cyclohexene of covalently grafted Fe(III)-complexes formed with various or various combinations of C-protected amino acid (L-histidine, L-tyrosine, L-cysteine and L-cystine) ligands are presented. The structural features of the surface complexes were studied by XANES/EXAFS and mid/far-IR spectroscopies. The compositions of the complexes were determined by ICP-MS and the Kjeldahl method. The SOD activities of the materials were evaluated in a biochemical test reaction. The obtained materials were used as catalysts for the oxidation of cyclohexene with peracetic acid in acetone. Both covalent grafting and building the complex onto the surface of the chloropropylated silica gel were successful in most cases. In many instances, the obtained structures and the coordinating groups were found to substantially vary upon changing the conditions of the syntheses. All the covalently immobilized Fe(III)-complexes displayed SOD activities, and most of them were found to be capable of catalyzing the oxidation of cyclohexene with appreciably high activities and outstanding epoxide selectivities.

G. Varga · Z. Csendes · I. Pálinkó (✉)
Department of Organic Chemistry, University of Szeged, Dóm tér 8, Szeged 6720, Hungary
e-mail: palinko@chem.u-szeged.hu

G. Varga · Z. Csendes · É. G. Bajnóczi · P. Sipos · I. Pálinkó
Material and Solution Structure Research Group, Institute of Chemistry, University of Szeged, Dóm tér 7-8, Szeged 6720, Hungary

É. G. Bajnóczi · P. Sipos
Department of Inorganic and Analytical Chemistry, University of Szeged, Dóm tér 7, Szeged 6720, Hungary

S. Carlson
MaxIV-Lab, Lund University, 223 63 Lund, Sweden

Published online: 05 February 2015

Keywords Silica-anchored · Fe(III)-C-protected amino acids · Covalent anchoring · Structural characterization · Catalytic activity and selectivity

Introduction

Enzymes catalyze a wide range of chemical transformations. They often provide high regio- and stereoselectivity and operate under physiological conditions. Enzyme-catalyzed reactions can be alternatives to traditional organic syntheses under environmentally benign conditions [1]. Outside the usual physiological environment, such as temperatures higher than the physiological, pH, or presence of non-aqueous solvents, enzymes are unstable and are easily inactivated. Therefore, they have several limitations for broader applications like catalysts in the synthesis of fine chemicals. Moreover, the recovery and the reuse of enzymes are also cumbersome. These drawbacks can be eliminated and more stable and reusable catalysts may be produced by immobilizing the enzyme over various supports by employing methods that preserve the catalytic activity and selectivity of the support-free enzyme [2, 3].

Active and selective solid catalysts can also be fabricated by immobilizing either the active site itself, or its structural or functional model [4]. Both approaches are applied in various laboratories, and promising results emerge. These biomimetic catalysts comprise redox-active transition metal ions [5] complexed by amino acids [6], or other molecules that are capable of coordination [7]. The immobilized complexes are often called bioinspired catalysts, and their activities and selectivities may resemble those of the enzymes. These substances are capable of operating under more rigorous conditions, and they can easily be recovered and recycled [8].

In this contribution, the active center of the Fe(III) superoxide dismutase (SOD) enzyme was used for inspiration [9]. It appears in the form of dimers or tetramers with one Fe ion per monomer unit and with a molecular weight of 22 kDa. The geometry around the metal ion is trigonal bipyramidal, coordinated by two histidine and one aspartate ligands in the equatorial plane and a histidine and a solvent molecule in the axial plane. The solvent molecule, which is OH^- in the oxidized and H_2O in the reduced form of the enzyme, is supported by an extensive network of H-bonds [10, 11].

There is hope to obtain efficient, durable, and recoverable electron transfer catalysts that can be reused, if one can immobilize the functional mimics of this enzyme in one way or another (e.g., hydrogen bonding, ion exchange, covalent anchoring) on solid supports of various kinds (e.g., zeolites, layered materials, resins, unmodified or surface-modified silica gel). This hope is supported by a range of literature results [12–17].

Catalytic epoxidation of alkenes by various oxidants is of interest, since epoxides are intermediates and precursors to many useful chemical products [18], such as food additives, agrochemicals, drugs, [19] perfumes, and sweeteners [20]. Cyclohexene oxide is used in the synthesis of many products, e.g., chiral pharmaceuticals, epoxy paints, pesticides, dyestuffs, and rubber promoters [21, 22].

Mainly hydrogen peroxide, organic peroxides (*tert*-butyl hydroperoxide), peracids (peracetic acid, *m*-chloroperbenzoic acid), and molecular oxygen are used as oxidants for oxidation of alkenes [23–25].

Peracids can epoxidize alkenes without adding catalyst; however, for the uncatalyzed reaction, relatively high reaction temperatures and long reaction times are needed [26]. These drawbacks can be eliminated by adding transition metal catalyst to the reaction [27].

In the following section, a summary is given based on previously published results [28, 29], on the construction, some aspects of structural characterization and SOD-like activity testing of Fe(III)-C-protected uniform or mixed amino acid complexes covalently anchored onto chloropropylated silica gel, inspired by the active centre of the FeSOD enzyme, and an account is provided on these features of newly constructed silica-anchored complexes. Furthermore, the hitherto unpublished results concerning the catalytic activities and selectivities of all these anchored complexes are also communicated here.

Experimental

Materials and methods of syntheses

For the syntheses, C-protected (in the form of methyl ester) L-histidine, L-tyrosine, L-cysteine, and L-cystine were used as ligands. The metal ion source was $FeCl_3 \cdot 6H_2O$. Chloropropylated silica gel (SG particle size, 230–400 mesh, BET surface area, 500 m^2/g, functionalization, 8 %)] was used as support. These materials as well as the 2-propanol solvent were products of Aldrich Chemical Co. All chemicals were of analytical grade and were used without further purification.

The general features of the syntheses are as follows. The first step of immobilization was the reaction of the appropriately protected amino acid (1.75 mmol) and the support (0.5 g, containing 0.35 mmol of chlorine atoms). The C-protected amino acids were covalently grafted onto the support through N-alkylation like reaction by refluxing the mixture in 2-propanol (60 cm^3) under alkaline conditions. After 24 h, the solid substance was filtered, washed several times in order to remove the uncoupled amino acid excess, and then dried. Complexation followed the anchoring: the grafted support was soaked in the 2-propanolic (60 cm^3) solution of the metal salt (1.75 mmol) under continuous stirring at room temperature for 24 h. After filtering and washing, the obtained material was divided into two parts, and then half of it was set aside. This is what we call *covalent grafting under ligand-poor conditions*, i.e., only the immobilized protected amino acids were available for coordination. To the other half, 2-propanolic (60 cm^3) solution of the appropriately protected amino acid derivative was added in excess (0.875 mmol), and the suspension was continuously stirred at room temperature for 24 h. Then, the solid material was filtered, rinsed with 2-propanol several times, and dried. The latter was named *covalent grafting under ligand-excess conditions*, i.e., the surface–grafted complex might have rearranged in the presence of excess amino acid mixture.

Surface–grafted complexes were prepared having both uniform and mixed amino acid derivatives (two protected amino acids were used) as ligands. Two methods were applied for the syntheses when mixed ligands were used. In method '*A*', one of the protected amino acid esters was covalently anchored to the surface of the support; then, it was soaked in the metal salt solution, and after filtering and thorough washing, the final substance was made by allowing complexation with excess amounts of the other amino acid ester. In method '*B*' a 1:1 molar mixture of the protected amino acids was grafted onto the surface of the support; then, the metal complex was formed. Parts of the materials thus formed were further treated in excess 1:1 protected amino acid mixtures resulting in the formation of surface-anchored complexes under ligand-excess conditions. The other experimental parameters were the same as described earlier.

The materials used in structural characterization and for catalytic testing together and their codes used in the followings are listed as follows:

SG–Tyr-OMe–Fe(III)[a]
SG–*Cys*-OMe–Fe(III), complex made under ligand-poor conditions
SG–*Cys*-OMe–Fe(III)–H-*Cys*-OMe, complex made under ligand-excess conditions
SG–(*Cys*-OMe)$_2$–Fe(III),
SG–(*Cys*-OMe)$_2$–Fe(III)M–H-(*Cys*-OMe)$_2$,
SG–His-OMe–Fe(III)–H-*Cys*-OMe[b], complex made with method '*A*'
SG–*Cys*-OMe–Fe(III)–H-His-OMe[b],
SG–His-OMe;*Cys*-OMe–Fe(III)[b], complex made with method 'B', under ligand-poor conditions
SG–His-OMe;*Cys*-OMe–Fe(III)–H-His-OMe;H-*Cys*-OMe[b], complex made with method 'B' under ligand-excess conditions
SG–His-OMe–Fe(III)–(H-*Cys*-OMe)$_2$,
SG–(*Cys*-OMe)$_2$–Fe(III)–H-His-OMe,
SG–His-OMe;(*Cys*-OMe)$_2$–Fe(III),
SG–His-OMe;(*Cys*-OMe)$_2$–Fe(III)–H-His-OMe;(H-*Cys*-OMe)$_2$.

a, b—Synthesis, structural characterization and SOD-like activity is described in Refs. [28, 29], respectively.

Analytical measurements

The amount of Fe(III) ions on the surface-modified silica gel was measured by an Agilent 7,700× ICP-MS. Before measurements, a few milligrams of the anchored complexes measured by analytical accuracy were digested in 1 cm^3 cc. H_2SO_4; then, they were diluted with distilled water to 50 cm^3 and filtered. The possibility of metal ion leaching was also studied by the ICP-MS method with the same instrument.

The nitrogen content of the samples was determined by the Kjeldahl method (the composition of the reaction mixture: 5 cm^3 cc. H_2SO_4, 1 cm^3 30 % solution of H_2O_2, 100 mg of the grafted complexes).

X-ray absorption spectroscopy (XAS) measurements

The measurements were carried out on the K-edge of the metals at MAX-lab at beamline I811. This is a superconducting multipole wiggler beamline equipped with a water-cooled channel cut Si(111) double crystal monochromator delivering at 10 keV, approximately 2×10^{15} photons/s/0.1 % bandwidth with horizontal and vertical FWHM of 7 and 0.3 mrad, respectively [30]. A beamsize of 0.5 mm × 1.0 mm (width × height) was used. The incident beam intensity (I_0) was measured with an ionization chamber filled with a mixture of He/N_2. Higher-order harmonics were reduced by detuning the second monochromator to 50–70 % of the maximum intensity, depending on the metal. Data collection was performed in transmission mode. Samples (~300 mg) were measured in Teflon spacers with Kapton tape windows.

XAS spectra were normalized to an edge jump of unity and the background absorption was removed.

The EXAFS data were k^3-weighted and Fourier transformed in the range of $k = 2$–12 Å^{-1}. The ranges for the backtransform were 1–3 Å for all complexes. The fitted parameters included the amplitude reduction factor (S_0^2), interatomic distances (R), Debye–Waller factors (σ^2), and energy shift (ΔE_0). The coordination numbers (N) were kept constant during each optimization, but a range of coordination numbers were used to find the best fit.

The main objectives of these measurements were to determine the coordination numbers, geometries around the Fe(III) ion, and to find out whether the sulphur atom was coordinated to the central ion in the anchored Fe(III) complexes.

Mid/far range FT-IR spectroscopy

Structural information on each step of the synthesis procedure was obtained by far- and mid-range infrared spectroscopy. Mid-range spectra were recorded with a BIO-RAD Digilab Division FTS-65 A/896 FT-IR spectrophotometer with 4 cm^{-1} resolution, measuring diffuse reflectance. A total of 256 Scans were collected for each spectrum; 300 mg KBr and 10 mg sample were combined and finely ground. Spectra were evaluated by the Win-IR package. They were baseline-corrected, smoothed (if it was necessary), and the spectra of the supports were subtracted. The 3,800–600 cm^{-1} wavenumber range was investigated. The comparison of the difference mid-IR spectra of the anchored amino acid derivatives with and without metal ion and the spectra of the pristine amino acid derivatives gives indirect information on the coordinating groups. The difference Δ [$\Delta = \nu_{asym(COO-)} - \nu_{sym(COO-)}$] between the asymmetric and symmetric carboxylate vibrations gives information about the coordination mode of the carboxylate group. The coordination can be either bidentate chelating ($\Delta_{complex} < \Delta_{ligand}$) or bidentate bridging ($\Delta_{complex} \sim \Delta_{ligand}$) or monodentate ($\Delta_{complex} > \Delta_{ligand}$) [31]. A shift in the position of the carbonyl group and the phenolic C–O or the absence of the S–H stretching vibration indicates the participation of these groups in complexation [32, 33].

Far-range spectra were recorded with a BIO-RAD Digilab Division FTS-40 vacuum FT-IR spectrophotometer with 4 cm^{-1} resolution. A total of 256 scans were collected for each spectrum. The Nujol mull technique was used between two

polyethylene windows (the suspension of 10 mg sample and a drop of Nujol mull). Spectra were evaluated by the Win-IR package. They were baseline-corrected and smoothed (if it was necessary). Unfortunately, in several cases the spectra could not be used for evaluation. The spectra in the far-IR region provide direct information on metal ion–functional group coordination, although assignation of the vibrations is not a trivial exercise. For making it easier, probe complexes having uniform, thus easily identifiable, coordinating groups were prepared and their far-IR spectra were registered. Fe(III)-complexes of imidazole, isopropylamine, and monosodium malonate were prepared. Each probe complex was synthesized via using 2-propanol (10 cm^3) as solvent. The metal salt (4×10^{-4} mol) and the ligand (2.4×10^{-3} mol) were stirred for 24 h at room temperature to get a solid precipitate. The obtained materials were filtered and washed with 2-propanol.

Testing the superoxide dismutase activity

The SOD activity was tested by the Beauchamp–Fridovich reaction [34]. A brief description of this biochemical test reaction is as follows. For this reaction, riboflavin, L-methionine, and nitro blue tetrazolium were used. Under aerobic conditions, reaction takes place on illumination between riboflavin and L-methionine. It is a reduction, and the reduced form of riboflavin reacts with oxygen forming a peroxide derivative. This derivative decomposes giving the superoxide radical anion. This radical ion is captured by the nitro blue tetrazolium (NBT) and its original yellow color turns blue.

The transformation can be followed by Vis spectrophotometry, measuring the absorbance at 560 nm. If our enzyme-mimicking material works well, it successfully competes with NBT in capturing the superoxide radical ion. Thus, the photoreduction of NBT is inhibited. The SOD probe reaction was carried out at room temperature in a suspension of the immobilized complex at pH = 7 ensured with a phosphate or for the Mn(II) complexes, 4-(2-hydroxyethyl)-1-piperazineethanesulfonic acid (HEPES) buffer. The reaction mixture contained 0.1 cm^3 of 0.2 mM riboflavin, 0.1 cm^3 of 5 mM NBT, 2.8 cm^3 of 50 mM buffer, containing EDTA (0.1 mM), L-methionine (13 mM), and the catalyst. Riboflavin was added last, and the reaction was initiated by illuminating the tubes with two 15-W fluorescent lamps. Equilibrium could be reached in 10 min. EDTA masks the interfering metal ion traces, since the metal ion–EDTA complexes have no SOD activity. From the resulting graph, the volume of enzyme-mimicking complex corresponding to 50 % inhibition (IC_{50}) was registered to allow a comparison with the efficiency of the real enzyme and other SOD mimics. The enzyme mimic works the better when the IC_{50} is the smaller. There was no reaction without illumination, and the support did not display SOD activity either.

Catalytic oxidation of cyclohexene

In the reaction, a vial with septum was loaded with the catalyst (25 mg), acetone (10 ml), cyclohexene (5 mmol), and 2.5 mmol peracetic acid ($\sim$39 % in acetic

acid). After 3 h of continuous stirring at room temperature, the mixture was analyzed quantitatively with a Hewlett-Packard 5,890 Series II gas chromatograph (GC) using an Agilent HP-1 column and the internal standard technique. The temperature was increased in stages from 50 to 250 °C. The products were identified via the use of authentic samples.

Results and discussion

Analytical measurements

The results of the Kjeldahl method and the ICP-MS measurements for the grafted Fe(III)-complexes containing uniform ligands are displayed in Table 1.

In all cases, the metal ion-to-amino acid ratios indicate (they are never integers) that mixtures of various kinds of complexes were formed on the surface. The amino acid content of SG–Tyr-OMe–Fe(III) and SG–Tyr-OMe–Fe(III)–H-Tyr-OMe is almost the same, suggesting (just as the mid-IR spectra published in Ref. [28]) that the preparation of the complex under ligand-excess conditions was not successful.

X-ray absorption measurements

Fe K-edge XAS spectra were recorded for some complexes formed with sulphur-containing ligands. The XANES spectra of the materials are depicted in Fig. 1.

Since the local symmetry around the Fe is higher in octahedral than in tetrahedral complexes, the intensity of the characteristic pre-edge peak around 7,113 eV decreases in the following order: $I_{\text{tetrahedral}} > I_{\text{square pyramidal}} > I_{\text{octahedral}}$ [35]. Comparison of the normalized intensity of the pre-edge peak in the anchored Fe(III)-complexes ($I \sim 0.05$) with that of some reference compounds indicates that the complexes are 5-coordinate; they are square pyramidal [35].

The Fourier-transformed EXAFS data (without phase correction) are displayed in Fig. 2, and the results of the fitting are shown in Table 2.

Table 1 Amino acid and Fe^{3+} content of the samples obtained from Kjeldahl type N-determination and ICP-MS measurements

Sample	Amino acid content (mmol/g)	Fe^{3+} content (mmol/g)
SG–Tyr-OMe–Fe(III)[a]	0.572	0.380
SG–Tyr-OMe–Fe(III)–H-Tyr-OMe[a]	0.581	0.382
SG–*Cys*-OMe–Fe(III)	0.460	0.333
SG–*Cys*-OMe–Fe(III)–H-*Cys*-OMe	0.654	0.333
SG–(*Cys*-OMe)$_2$–Fe(III)	0.445	0.370
SG–(*Cys*-OMe)$_2$–Fe(III)–H-(*Cys*-OMe)$_2$	0.924	0.371

[a] Their syntheses and mid-IR characterization was published in Ref. [28], but Kjeldahl measurements were not performed then

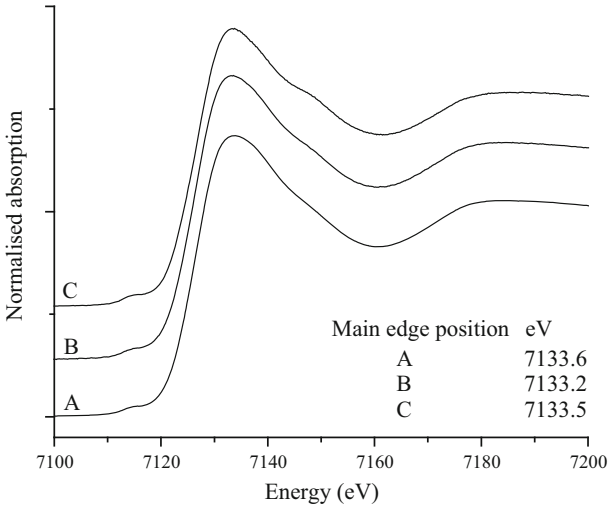

Fig. 1 The Fe K-edge XANES spectra of *A*—SG–(*Cys*-OMe)$_2$–Fe(III), *B*—SG–*Cys*-OMe–Fe(III) and *C*—SG–His-OMe–Fe(III)–H-*Cys*-OMe

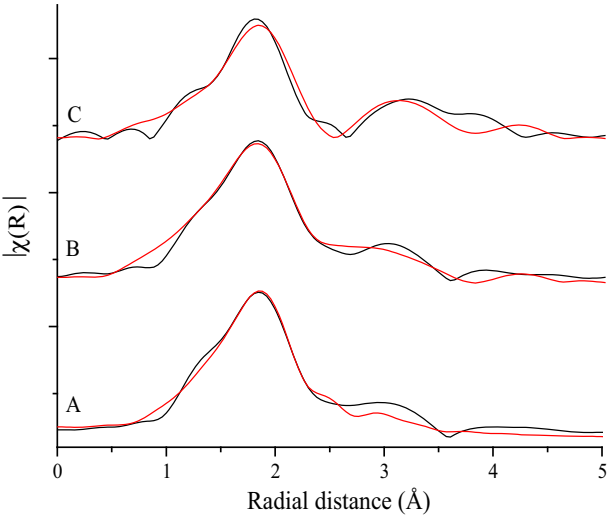

Fig. 2 The Fourier-transformed EXAFS data (without phase correction) of *A*—SG–(*Cys*-OMe)$_2$–Fe(III), *B*—SG–*Cys*-OMe–Fe(III) and *C*—SG–His-OMe–Fe(III)–H-*Cys*-OMe, *red line*—fit, *black line*—experimental. (Color figure online)

In the first coordination shell of SG–(*Cys*-OMe)$_2$–Fe(III), there are five oxygen/nitrogen atoms, with a Fe(III)–O/N bond length of 1.98 Å. For SG–*Cys*-OMe–Fe(III), the first coordination sphere contains four O/N atoms and one sulphur atom, where the bond distances were fitted to be 1.98 and 2.36 Å, respectively. In SG–

Table 2 Parameters deduced from the fitted EXAFS spectra

Sample	(Fe^{3+}–)X	*N*	*R* (Å)	σ^2 (Å^2)	ΔE_0 (eV)	*R* factor
SG–(*Cys*-OMe)$_2$–Fe(III)	O/N	5	1.98	0.0080	−1.44	0.0179
SG–*Cys*-OMe–Fe(III)	O/N	4	1.98	0.0120	−5.37	0.0135
	S	1	2.36	0.0327		
SG–His-OMe–Fe(III)–H-*Cys*-OMe	O/N	3.6	1.98	0.0114	−5.69	0.0120
	S	1.4	2.36	0.0232		

N—coordination number, *R*—bond length, σ^2—Debye–Waller factor, ΔE_0—energy shift, *R* factor—goodness of fit

His-OMe–Fe(III)–H-*Cys*-OMe, the Fe(III)–O/N distance is 1.98 Å and the average coordination number is 3.6, while for Fe(III)–S, these date are 2.36 Å and 1.4, respectively. The thiolate sulphur donor atom is coordinated to the Fe(III) irrespective to whether the cysteine is anchored or non-anchored on the surface of the support.

Mid/far-range FT-IR spectroscopy

As far as SG–*Cys*-OMe–Fe(III) is concerned (Fig. 3, trace A), the carboxylate group is most probably coordinated as monodentate ligand, since Δ increased from 190 to 216 cm^{-1} (1,602–1,386 cm^{-1}). The XAS measurement revealed the coordination of

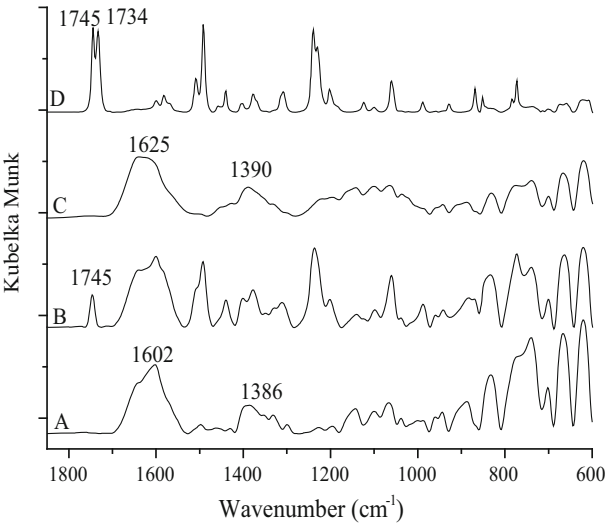

Fig. 3 The difference IR spectra of *A*—SG–*Cys*-OMe–Fe(III), *B*—SG–*Cys*-OMe–Fe(III)–H-*Cys*-OMe, *C*—SG–(*Cys*-OMe)$_2$–Fe(III) and *D*—SG–(*Cys*-OMe)$_2$–Fe(III)–(H-*Cys*-OMe)$_2$ (the spectrum of the support was subtracted)

the thiolate sulphur, and the lack of the S–H vibration further confirms that. Under ligand-excess conditions (Fig. 3, trace B), the carbonyl oxygen is not involved in the coordination, since the stretching vibration of the carbonyl band did not shift to lower wavenumbers (1,745 cm^{-1}). There is no S–H vibration at around 2,500 cm^{-1}; therefore, the thiolate sulphur is coordinated.

For the SG–(*Cys*-OMe)$_2$–Fe(III), $\Delta = 1{,}625 - 1{,}390\ cm^{-1} = 235\ cm^{-1}$ suggesting the monodentate ligation of the carboxylate groups (Fig. 3, trace C). Under ligand-excess conditions (Fig. 3, trace D), the carbonyl oxygens do not take part in the complexation, since the positions of the bands (1,745, 1,734 cm^{-1}) do not move relative to the pristine amino acid.

In the far-IR range (Fig. 4, trace A), the bands at 383 and 294 cm^{-1} correspond to the Fe(III)–N_{amino} vibrations.

Using all these pieces of information structural proposals for the surface–bound complexes are offered as follows:

SG–*Cys*-OMe–Fe(III)

$$S_{thiolateCyssurf}O_{carboxylateCysssurf}H_2O, H_2O, H_2O,$$

SG–*Cys*-OMe–Fe(III)–H-*Cys*-OMe

$$S_{thiolateCyssurf}O_{carboxylateCysssurf}S_{thiolateCys}S_{thiolateCys}H_2O,$$

SG–(*Cys*-OMe)$_2$–Fe(III)

$$O_{carboxylate(Cys)2surf}O_{carboxylate(Cys)2surf}H_2O, H_2O, H_2O,$$

SG–(*Cys*-OMe)$_2$–Fe(III)–(H-*Cys*-OMe)$_2$

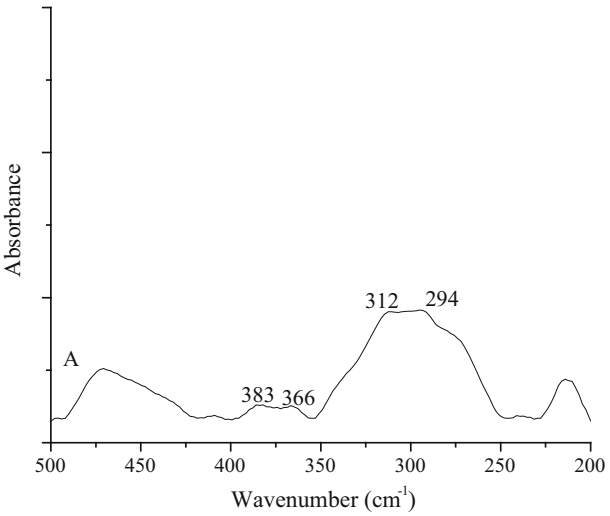

Fig. 4 The difference far-IR spectra of *A*—SG–(*Cys*-OMe)$_2$–Fe(III)–(H-*Cys*-OMe)$_2$ (the spectrum of the support was subtracted)

$$O_{carboxylate(Cys)2surf}O_{carboxylate(Cys)2surf}N_{amino(Cys)2}N_{amino(Cys)2}H_2O.$$

SG–His-OMe–Fe(III) was rearranged by adding C-protected cystine in excess (Fig. 5, trace A). The stretching vibration of the carbonyl band (1,739 cm^{-1}) did not move relative to the free C-protected cysteine; therefore, it can only coordinate with the amino nitrogens.

In Fig. 5, trace B depicts the spectrum of SG–(*Cys*-OMe)$_2$–Fe(III)–H-His-OMe. The spectrum is very similar to that of the C-protected histidine—the carbonyl oxygen does not participate in the complexation.

In SG–His-OMe;(*Cys*-OMe)$_2$–Fe(III), the anchored amino acids are again assumed to coordinate as they did alone (Fig. 5, trace C).

Under ligand-excess conditions (Fig. 5, trace D), three unshifted carbonyl vibrations can be seen at 1,760 (C-protected histidine), 1,746 and 1,734 cm^{-1} (C-protected cystine).

Unfortunately, their far-IR spectra are unusable, but on the basis of these observations and the accumulated knowledge described at the complexes formed with uniform ligands, the following structures may be proposed:

SG–His-OMe–Fe(III)–(H-*Cys*-OMe)$_2$

$$N_{imidazoleHissurf}O_{carboxylateHissurf}N_{amino(Cys)2}N_{amino(Cys)2}H_2O,$$

SG–(*Cys*-OMe)$_2$–Fe(III)–H-His-OMe

$$O_{carboxylate(Cys)2surf}O_{carboxylate(Cys)2surf}N_{imidazoleHis}N_{imidazoleHis}H_2O,$$

SG–His-OMe;(*Cys*-OMe)$_2$–Fe(III)

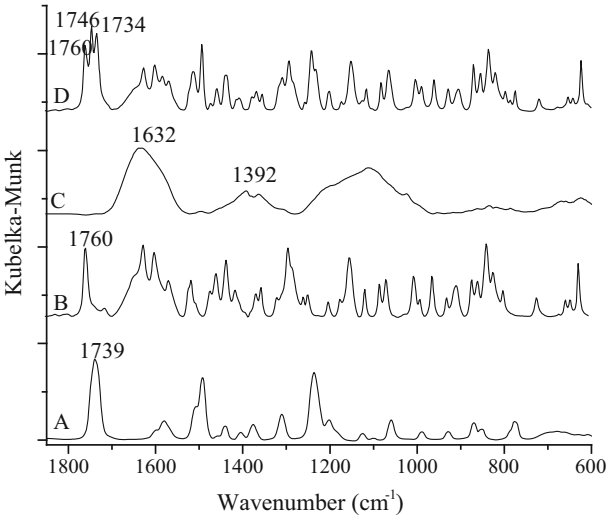

Fig. 5 The difference IR spectra of *A*—SG–His-OMe–Fe(III)–(H-*Cys*-OMe)$_2$, *B*—SG–(*Cys*-OMe)$_2$–Fe(III)–H-His-OMe, *C*—SG–His-OMe;(*Cys*-OMe)$_2$–Fe(III), *D*—SG–His-OMe;(*Cys*-OMe)$_2$–Fe(III)–H-His-OMe;(H-*Cys*-OMe)$_2$ (the spectrum of the support was subtracted)

$$N_{imidazoleHissurf}O_{carboxylateHissurf}O_{carboxylate(Cys)2surf}O_{carboxylate(Cys)2surf}H_2O,$$

SG–His-OMe;(*Cys*-OMe)$_2$–Fe(III)–H-His-OMe;(H-*Cys*-OMe)$_2$

$$N_{imidazoleHissurf}O_{carboxylateHissurf}O_{carboxylate(Cys)2surf}N_{imidazoleHis}N_{amino(Cys)2}.$$

Superoxide dismutase activity of the complexes

All materials were active in catalyzing the dismutation reaction of the superoxide radical anion. Catalytic activities differed widely though (Table 3).

Data reveal that there were catalysts with activity close to that of the Cu,ZnSOD enzyme. The most active substances contain cysteine, indicating the key role of cysteine-like structures in determining catalytic activity. They seem to have the optimum structures for promoting this reaction. SG-Tyr-OMe-Fe(III) was the second most active material, in which tyrosine coordinates as tridentate ligand, making the complex more strained.

Catalytic oxidation of cyclohexene

The catalytic oxidation of cyclohexene takes place according to Scheme 1 [36].

After performing numerous optimization experiments, we found that for our supported Fe(III) complexes, 3 h reaction time and 2.5 mmol peracetic acid were needed to obtain the highest epoxide selectivity, and the reactions must have been performed in acetone to avoid the decomposition of the oxidant.

Table 3 The SOD activities of the surface-grafted complexes

Materials	IC_{50} (μM)
Cu,ZnSOD enzyme	0.4
SG–Tyr-OMe–Fe(III)[a]	5
SG–*Cys*-OMe–Fe(III)	6
SG–*Cys*-OMe–Fe(III)–H-*Cys*-OMe	31
SG–(*Cys*-OMe)$_2$–Fe(III)	36
SG–(*Cys*-OMe)$_2$–Fe(III)–H-(*Cys*-OMe)$_2$	33
SG–His-OMe–Fe(III)–H-*Cys*-OMe[b]	28
SG–*Cys*-OMe–Fe(III)–H-His-OMe[b]	25
SG–His-OMe;*Cys*-OMe–Fe(III)[b]	21
SG–His-OMe;*Cys*-OMe–Fe(III)–H-His-OMe;H-*Cys*-OMe[b]	4
SG–His-OMe–Fe(III)–(H-*Cys*-OMe)$_2$	24
SG–(*Cys*-OMe)$_2$–Fe(III)–H-His-OMe	32
SG–His-OMe;(*Cys*-OMe)$_2$–Fe(III)	31
SG–His-OMe;(*Cys*-OMe)$_2$–Fe(III)–H-His-OMe;(H-*Cys*-OMe)$_2$	28

[a,b] Data published in Refs. [28, 29], respectively, are shown for comparison

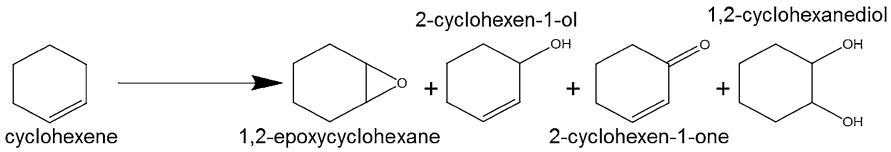

Scheme 1 The oxidative transformations of cyclohexene

Table 4 The conversion and selectivity results of the oxidation of cyclohexene after 3 h; the best catalysts are highlighted in *italics*

Catalyst	Conversion (%)	Epoxide (%)	Alcohol (%)	Ketone (%)	Diol (%)
–	21	64	4	2	30
SG–Tyr-OMe–Fe(III)	45	94	2	1	3
SG–*Cys*-OMe–Fe(III)	59	87	3	8	2
SG–Cys-OMe–Fe(III)–H-Cys-OMe	*56*	*99*	*1*	*0*	*0*
SG–(*Cys*-OMe)$_2$–Fe(III)	25	97	1	1	1
SG–(*Cys*-OMe)$_2$–Fe(III)–H-(*Cys*-OMe)$_2$	10	95	2	1	2
SG–His-OMe–Fe(III)–H-*Cys*-OMe	44	88	2	0	10
SG–*Cys*-OMe–Fe(III)–H-His-OMe	65	85	2	9	4
SG–His-OMe;Cys-OMe–Fe(III)	*49*	*98*	*1*	*0*	*1*
SG–His-OMe;Cys-OMe–Fe(III)–H-His-OMe;H-Cys-OMe	*32*	*97*	*1*	*1*	*1*

Initially, for activity (and selectivity) testing, three selection criteria were applied. First, those complexes were chosen, which displayed high activities in the biochemical reaction; second, their "pairs" (syntheses under ligand-poor—ligand excess conditions) were included (if they existed); and third, complexes constructed by all varieties must be represented.

The activity and selectivity data in Table 4 attest that all the chosen immobilized complexes were catalytically active, and that the major product of the reactions was the epoxide. It is to be seen that in many cases, the conversion of catalyzed reaction was significantly higher than that of the stoichiometric. The cystine-containing complexes only had lower conversions than the stoichiometric reaction; therefore, all the other cystine-containing complexes were excluded from the tested catalyst group. The selectivities, which were very significantly higher for the catalyzed reaction than for the stoichiometric one, virtually did not depend on the identity of the amino acid ligand. The presence of the ligands was necessary though, since silica gel impregnated with the Fe(III) ions only decomposed the peracetic acid.

Concerning epoxide selectivity *and* catalytic activity, the best catalyst is SG–*Cys*-OMe–Fe(III)–H-*Cys*-OMe with 99 and 56 % selectivity and conversion, respectively. In general, cystine-containing materials did not catalyze this reaction well (but the epoxide selectivities are still high), moreover, for SG–(*Cys*-OMe)$_2$–

Fe(III)–H-(*Cys*-OMe)$_2$ the observed conversion was lower than that of the homogeneous, uncatalyzed reaction.

Leaching of the metal ion was not observed, and the catalysts, highlighted in italics in Table 4, could be reused twice just after rinsing it with the solvent.

The mechanism of the reaction is suggested as follows: one of the coordinated water molecules is replaced by the peroxidic oxygen donor oxidant, forming (hydro)peroxo-metal species, then, the O–O bond is cleaved heterolytically to form high-valent metal-oxo species as an active intermediate, which is responsible for the epoxidation of the uncoordinated cyclohexene. If both reactants were coordinated, there would be plenty of time for further reactions. If cyclohexene was coordinated alone, the situation would not be much different from the stoichiometric reaction. Thus, probably, the role of the ligands is to exert steric influence on the accessibility of the central ion by the reactants.

Conclusions

All the SOD-mimicking surface-anchored Fe(III)–amino acid complexes were successfully constructed. It was possible to prepare the covalently anchored complexes with uniform and mixed ligands as well. Covalent anchoring gave good control over the mode of immobilization.

Analytical measurements revealed that mixtures of complexes with 1:1, 1:2, and 1:3 metal ion-to-ligand ratios were formed on the surface of the support. The coordination numbers and coordinating sites could be identified with the combination of XAS measurements, mid- and far-IR spectroscopies and chemical considerations. It was proven that the Fe(III) complexes were square pyramidal. The major coordinating sites were proposed to be the carboxylate oxygen, the imidazole nitrogen, the phenolate oxygen and sulphur atom of the thiolate group. The other coordination sites depended on the conditions of the synthesis and the structures of the molecules. In all cases, water molecules saturated the coordination sphere. In most cases under ligand–excess conditions, the surface–anchored ligand–poor complexes were rearranged.

All the covalently anchored complexes were active in a SOD test reaction: they could catalyze the dismutation reaction of the superoxide radical anion. The activity, in some cases, was only one magnitude lower that of the native Cu,ZnSOD enzyme.

The complexes displayed catalytic activity in the oxidation of cyclohexene, and all of them were extremely selective to cyclohexene oxide formation. Some of the best catalysts were reused twice without significant loss in the catalytic activity and selectivity. The activities were, but the selectivities were basically not dependent on the coordinating groups.

Immobilization of transition metal–amino acid complexes turned out to be a viable route for preparing efficient electron transfer catalysts, since they are very active and selective catalysts that can be easily recovered and recycled. They show the promise of becoming efficient catalysts in the synthesis of fine chemicals.

Acknowledgments This research was financed by the TÁMOP 4.2.2.A-11/1/KONV-2012-0047 and the OTKA 83889 Grants. The support is highly appreciated.

References

1. K.M. Koeller, C.H. Wong, Nature **409**, 232 (2001)
2. U. Hanefeld, L. Gardossi, E. Magner, Chem. Soc. Rev. **38**, 453 (2009)
3. U.T. Bornscheuer, Angew. Chem. Int. Ed. **42**, 3336 (2003)
4. D.J. Xuereb, R. Raja, Catal. Sci. Technol. **1**, 517 (2011)
5. J.A. Labinger, J. Mol. Catal. A Chem. **220**, 27 (2004)
6. M. Luechinger, A. Kienhöfer, G.D. Pirngruber, Chem. Mater. **18**, 1330 (2006)
7. K. Suzuki, P.D. Oldenburg, L. Que Jr, Angew. Chem. Int. Ed. **47**, 1887 (2008)
8. B.M. Weckhuysen, J. Am. Chem. Soc. **128**, 3208 (2006)
9. A.-F. Miller, in *Handbook of Metalloproteins*, ed. by A. Messerschmidt, R. Huber, K. Wieghardt, T. Poulos (Wiley, Chichester, 2001), pp. 668–682
10. M.L. Ludwig, A.L. Metzger, K.A. Pattridge, W.C. Stallings, J. Mol. Biol. **219**, 335 (1991)
11. M.S. Lath, M.M. Dixon, K.A. Pattridge, W.C. Stallings, J.A. Fee, M.L. Ludwig, Biochem. **34**, 1646 (1995)
12. F. Farzaneh, S. Sohrabi, M. Ghiasi, M. Ghandi, V. Mehdi Ghandi, J. Porous Mater. **20**, 267 (2013)
13. M. Halma, K.A.D. de Freitas Castro, C. Taviot-Gueho, V. Prévot, C. Forano, F. Wypych, S. Nakagaki, J. Catal. **257**, 233 (2008)
14. A. Baso, L.D. Martin, C. Ebert, L. Gardossi, P. Linda, F. Sibilla, Tetrahedron Lett. **44**, 5889 (2003)
15. H.H.P. Yiu, P.A. Wright, J. Mater. Chem. **15**, 3690 (2005)
16. C. Ispas, I. Sokolov, S. Andreescu, Anal. Bioanal. Chem. **393**, 543 (2009)
17. G.D. Pirngruber, L. Frunz, M. Lüchinger, Phys. Chem. Chem. Phys. **11**, 2928 (2009)
18. Y. Zhang, J. Zhao, L. He, D. Zhao, S. Zhang, Mic. Mes. Mater. **94**, 159 (2006)
19. J. Gao, Y. Chen, B. Han, Z. Feng, C. Li, N. Zhou, Z. Gao, J. Mol. Catal., A **210**, 197 (2004)
20. S. Samantaray, K. Parida, Catal. Commun. **6**, 578 (2005)
21. S. Bhattacharjee, J.A. Anderson, J. Mol. Catal. A **249**, 103 (2006)
22. C. Marchi-Delapierre, A. Jorge-Robin, A. Thibon, S. Ménage, Chem. Commun. 1166 (2007)
23. J. Jiang, K. Ma, Y. Zheng, S. Cai, R. Li, J. Ma, Appl. Clay Sci. **45**, 117 (2009)
24. R. Noyori, M. Aoki, K. Sato, Chem. Commun. 1977 (2003)
25. T. Punniyamurthy, L. Rout, Coord. Chem. Rev. **252**, 134 (2008)
26. H. Shi, Z. Zhang, Y. Wang, J. Mol. Catal. A **238**, 13 (2005)
27. K.-P. Ho, W.-L. Wong, K.-M. Lam, C.-P. Lai, T.H. Chan, K.-Y. Wong, Chem. Eur. J. **14**, 7988 (2008)
28. Z. Csendes, Cs. Dudás, G. Varga, É.G. Bajnóczi, S.E. Canton, P. Sipos, I. Pálinkó, J. Mol. Struct. **1044**, 39 (2013)
29. Z. Csendes, N. Földi, J.T. Kiss, P. Sipos, I. Pálinkó, J. Mol. Struct. **993**, 203 (2011)
30. S. Carlson, M. Clausen, L. Gridneva, B. Sommarin, C.J. Svensson, J. Synchrotron Radiat. **13**, 359 (2006)
31. S.K. Papageorgiou, E.P. Kouvelos, E.P. Favvas, A.A. Sapadilis, G.E. Romanos, F.K. Katsaros, Carbohydr. Res. **345**, 469 (2010)
32. S.A. Abdel-Latif, H.B. Hassib, Y.M. Issa, Spectrochim Acta Part A **67**, 950 (2007)
33. T. Miura, T. Satoh, H. Takeuchi, Biochim. Biophys. Acta **1384**, 171 (1998)
34. C. Beauchamp, I. Fridovich, Anal. Biochem. **44**, 276 (1971)
35. P. Chutia, S. Kato, T. Kojima, S. Satokawa, Polyhedron **28**, 370 (2009)
36. G. Bilis, K.C. Christoforidis, Y. Deligiannakis, M. Louloudi, Catal. Today **157**, 101 (2010)